Soluble Rigid Poly(Imide-Siloxane)s: Synthesis, Characterization, and Structure-Property Relations

M. Srividhya, B. S. R. Reddy

Industrial Chemistry Laboratory, Central Leather Research Institute, Adyar, Chennai 600020, India

Received 29 July 2006; accepted 4 March 2007
DOI 10.1002/app.27683
Published online 1 April 2008 in Wiley InterScience (www.interscience.wiley.com).

ABSTRACT: Three different poly(imide-siloxane)s (PIS) containing rigid imide groups were synthesized by the reaction of amine end-capped imides to the siloxane backbone. These highly soluble amine terminated imides were synthesized by reacting fluorinated anhydride and three different amines (DDBP, DDM, DBP). The imides were grafted to the siloxane backbone by the epoxy group cleavage. All the polymers were obtained in quantitative yields with the inherent viscosities ranging from 0.32 to 0.45 dL/g. The polymers were characterized by FTIR, ^{1}H and ^{13}C NMR, and their thermal properties were studied. The DSC results showed two distinct glass transition temperatures demonstrating the existence of phase separation between the hard imide and soft siloxane groups. Polymeric membranes were prepared employing the coupling reaction between PIS and the polydimethylsiloxane matrix by varying the amount of incorporation of PIS. The membranes showed a high tensile strength of 82 MPa. The contribution of polar and dispersion component towards the total surface energy was studied by the contact angle measurements, and a reduction in surface tension of 15 mN/m was achieved with the fluorine containing PIS membrane. The study of the surface morphology was studied which confirmed the existence of phase separation in these systems. © 2008 Wiley Periodicals, Inc. J Appl Polym Sci 109: 565–576, 2008

Key words: films; morphology; polyimides; polysiloxanes; structure-property relations

INTRODUCTION

The polysiloxane component imparts a number of beneficial properties to the polymeric system including enhanced solubility, gas permeability, reduced water sorption, good thermal and ultraviolet stability, resistance to degradation in aggressive oxygen environment, impact resistance, and modified surface properties.[1,2] Despite these advantageous properties, poor mechanical properties, especially low-tensile strength of these polysiloxanes limit their application in various applications like gas permeability. To improve the mechanical properties without sacrificing the desired properties of siloxane polymers, many investigations have been reported on the synthesis and characterization of block, segmented, and side-chain siloxane polymers.[3–5]

On the other hand, aromatic polyimides are promising membrane materials because of their high-gas selectivity, low-thermal expansion, excellent mechanical properties, chemical and radiation resistance, and the possibility of accessing a rich variety of chemical structures via facile modifications of the precursor monomers.[6,7] Polysiloxanes and polyimides form the best combination to utilize their properties which compensates each other's drawbacks. The insertion of hard polyimide segment to the soft siloxane backbone causes large changes in their properties.[8,9]

Despite their many attractive properties, aromatic polyimides cannot be used for reacting with the siloxanes because of the difference in their polarity factors which hinders their solubility in a common solvent to synthesize poly(imide-siloxane)s (PIS). The rigid structures give high-glass transition temperatures or high-crystalline melting points which are responsible for the poor solubility and processability for the imide groups. Research has been directed toward working with inherently intractable polymers or modifying the polyimide structure to achieve a more flowable and soluble behavior. In response to the known limitations of some polyimides, there has been a great deal of research in modifying the structure to improve flow and moldability, while maintaining thermal stability and high-temperature mechanical properties, which are characteristic of aromatic polyimides. Generally, it has been demonstrated that reducing the stiffness of the polymer backbone or lowering the interchain interactions can improve melt flow and solubility. The approaches that have been taken to achieve these results include introducing an angular or flexible linkage into the

Correspondence to: B. S. R. Reddy (induchem2000@yahoo.com).

Contract grant sponsor: DST; contract grant number: SR/S1/PC-15/2003.

Journal of Applied Polymer Science, Vol. 109, 565–576 (2008)

backbone; introducing a kinked linkage (*meta*- and *ortho*-catenations) or an unsymmetrical and cardo (loop) structure; incorporating a large polar or nonpolar pendant bulky group along the polymer backbone; or disrupting the symmetry of the polymer chain via copolymerization. Flexible or angular units have also been introduced within the polymer backbone to inhibit interchain interactions, to lower phase transition temperatures, and thus promote solubility and flowability.[10–15]

Another approach to improve the processability of polyimides is to introduce a bulky pendant group such as an alkyl, perfluoroalkyl, phenyl, and phenoxy along the polymer backbone.[16–19] Solubility and flowability are enhanced because the bulky pendant group reduces the interchain interaction by eliminating the charge-transfer complex between chains through steric hindrance.[20] Typically, T_g and thermal stability can be maintained at high levels utilizing this method. Among the various groups, the fluorinated blocks are generally used to increase the chemical resistance and thermal properties and also to reduce the surface tension.[21,22]

Moreover, the use of fluorinated groups into the polyimide backbone improves the solubility in the polar solvents. In addition to enhanced solubility and processability, another advantage of introducing fluorinated groups is to yield the polymer systems with low-dielectric constant, high-thermal stability, and gas permeability.[23] While these new fluorinated PIS possess important practical aspects, they exhibit novel morphological and mechanical features as well.

If more durable membrane materials can be developed, they would be economically and environmentally attractive alternatives to the common gas separation techniques. One of our main obstacles to develop robust membrane materials was the difficulty in the synthesis of easily processable PIS for membrane casting. The main goal of this study is to prepare and characterize PIS that were soluble in common organic solvents, having excellent film-forming properties, without substantially decreasing the rigidity of the polyimide backbone structure.

EXPERIMENTAL

Materials and methods

Poly(methylhydrogensiloxane) (PHMS), molecular weight of 1900 was obtained from Lancaster synthesis and stored in a sealed container in an inert atmosphere. 4,4′-(Hexafluoroisopropylidene) dipthalicanhydride (6FDA), 4,4′-diamino-3,3′-dimethoxybiphenyl (DDBP), 4,4′-diaminodiphenylmethane (DDM), 4,4′-diaminobenzophenone (DBP), and hexachloroplatinic acid monohydrate were purchased from Lancaster, UK and used as such. Toluene and dimethylformamide (DMF) were dried over calcium hydride and freshly distilled before use.

Measurements

FTIR spectra were recorded on a Perkin–Elmer spectrophotometer. ^{1}H and ^{13}C spectra were recorded on JEOL 500 MHz spectrophotometer at room temperature using ^6d-DMSO solvent with TMS as an internal standard. DSC scans were obtained from NETZSCH-Geratebauv GmbH instrument at the heating rate of 10°C/min under nitrogen atmosphere from −120 to 220°C. Thermal stability was determined using thermogravimetric analyzer (STA 1500) at a heating rate of 10°C/min under nitrogen atmosphere.

The weight-average molecular weight of the oligomers was determined by gel permeation chromatography (JASCO model MX-2080-31) with a RI detector using PL gel columns in THF with a flow rate of 1 mL/min. The molecular weights were calculated with a calibration relative to polystyrene standards.

WAXD spectra were recorded using Philips model XPERT-PRO X-ray diffraction spectrometer with a scan range (2θ) from 5° to 75° in transmission mode. The X-rays (wavelength = 1.54 Å) were produced by Cu Kα source. The voltage and the current settings used to generate the X-rays were 40 kV and 30 mA, respectively.

The contact angles of the films have been measured at ambient temperature by Sessile drop method using a camera mounted on a microscope to record the drop image, using Digidrop (GBX) model goniometer with windrop software. Double distilled water and *n*-octadecane were used as solvents for the studies. Equilibrium contact angle was measured for a time period of 120 s depending on the stability of the drop. Average of the results obtained from three experiments was taken for contact angle measurements. The surface energy of the films was calculated using Young and Fowkes equation and the details of the experimental procedure are reported elsewhere.[24]

The density of the films was measured using the buoyancy technique.[25] A well-dried film sample was first weighed in air. It was then immersed in distilled water at room temperature, and the difference in weight upon immersion was determined. The volume of the sample was calculated from the weight difference of the measurements divided by the density of distilled water. From the weight in air and the volume, the density of the film was calculated. For each density measurement, three values were taken and the average was taken as the density. The standard deviation varied from 0.005 to 0.01 g/cm^3.

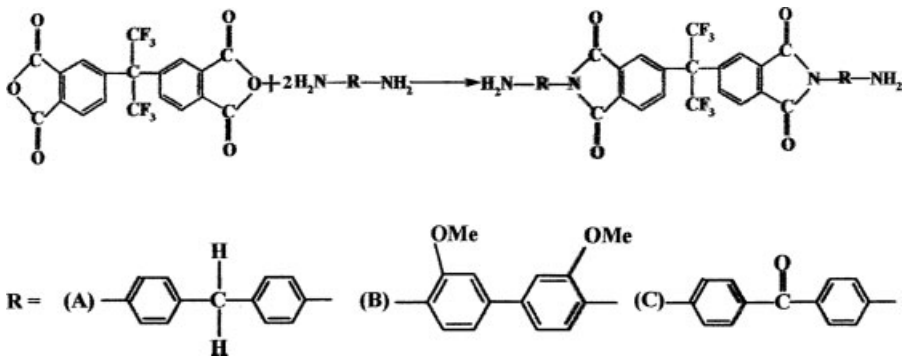

Scheme 1 Synthesis of amine end-capped imides.

The mechanical properties were determined using Micro Tensile Tester Instron 4501 at a speed of 10 mm/min. Dynamic mechanical thermal analysis (DMA) was performed using tensile mode form Universal V2.6D TA instrument at a heating rate of 10°C/min and a frequency of 1 Hz from −100°C. Scanning electron microscopy was done on Philips quanta 200 FEI. The samples were first sputtered with gold.

Synthesis of amine end-capped imides

The following procedure was carried out to synthesize all the three imides (A, B, and C) as mentioned in Scheme 1. 2.5 mmol (0.5 mol excess) of diamine was dissolved in 25 mL of DMF and stirred under nitrogen atmosphere at room temperature. Then, 1 mmol of 6FDA was slowly added in small portions with stirring. The reaction mixture was stirred for 2 h under inert atmosphere at room temperature. The solution imidization technique was carried out for 6 h using Dean-Stark apparatus by forming azeotropic mixture with toluene. The product formed was precipitated in the appropriate solvent which solubilizes the unreacted dianhydride and excess amine. Table I gives the elemental analysis data for the synthesized imides. The products were characterized by FTIR, ^{1}H and ^{13}C NMR.

FTIR for the imides (cm^{-1}): 3300 (free NH stretch); 1230 (C—N stretch); 3186 (Ar. CH); 842, 792 (Ar. ring substitution); 1586, 1421, 987 (Ar. ring breathing) 1321, 720 cm^{-1} (Ar. bending vibrations); 1724 (C=O in phase of imide); 1626 (C=O out of phase imide); 1315 (C—*N*—C of imide); 1250 (C—F); 2980, 1472 (—CH_2—).

^{1}H NMR (^{6}*d*-DMSO) ppm

A: 3.9 (4H, s), 4.0 (4H, s), 5.9–6.6 (8H, m), 7.5–7.9 (8H, m), 7.9–8.1 (6H, m); **B**: 3.3 (6H, s); 3.7 (6H, s); 3.8 (4H, s); 6–8 (18H, m); **C**: 3.5 (4H, s), 5.9–6.6 (8H, m), 7.5–7.9 (8H, m), 7.9–8.1 (6H, m).

In the ^{13}C NMR, the chemical shifts (ppm) that were observed in common for all the imides are as follows:

167 (—*N*—C=O imide), 112–133 (aromatic carbons), 123 (—CF_3), 64 (C—CF_3); **A**: 21.1 (CH_2); **B**: 154 (OCH_3); **C**: 163 (C=O).

Preparation of epoxy-functionalized siloxanes

Epoxy functionalized polydimethylsiloxane was synthesized as mentioned in Scheme 2 by adopting the procedure reported elsewhere.[26] About 1.9 g (1 mmol) of PHMS and 150 mL of dry toluene were taken in a 250-mL round bottom flask equipped with a Leibeigh condenser. To this, 2.86 g (25 mmol) of allyl-2-3-epoxypropylether was added and the solution was saturated with nitrogen gas prior to the addition of 0.5 mL containing 10^{-4} mmol of hexachloroplatinic acid in isopropanol solution. The mixture was heated at 80°C for 48–54 h and cooled to room temperature. It was stirred with activated charcoal to remove traces of platinum, filtered and the solvent along with other volatiles was removed under vacuum. The synthesized epoxy-functionalized PDMS were characterized by FTIR, ^{1}H and ^{13}C

TABLE I
Elemental Analysis Data of the Synthesized Amine-Terminated Imides

			C%		H%		N%	
Compound	Molecular formula	Mol. wt.	Calcd.	Found	Calcd.	Found	Calcd.	Found
A	$C_{45}H_{30}N_4O_4F_6$	803	67.25	67.01	3.73	3.57	6.97	6.86
B	$C_{47}H_{34}O_8N_4F_6$	896	62.95	62.21	3.79	3.34	6.25	6.09
C	$C_{45}H_{26}N_4O_6F_6$	831	64.98	64.09	3.13	2.98	6.74	6.56

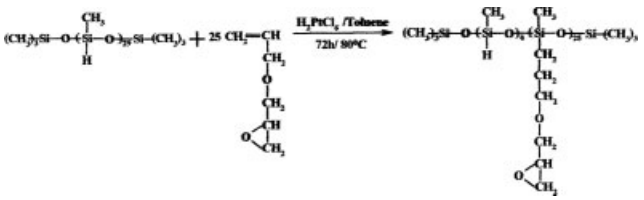

Scheme 2 Synthesis of epoxy-functionalized siloxanes.

NMR [Fig. 1(a–c)]. The epoxy equivalent weight (EEW) was obtained according to the reported procedure[27] and was found to be 216 g/mol. From the EEW and the integral ratio calculations from ^{1}H NMR between the SiH chemical shift at 4.6 ppm and epoxy at 3.3 ppm, the incorporation of the allyl group to PHMS was determined and found to be 22 groups.

Preparation of poly(imide-siloxane)s

Scheme 3 represents the incorporation of the amine-terminated imides to the PHMS backbone. All the synthesized imides were found to be highly soluble in DMF. Twenty-two millimolar of the imide was dissolved in 5 mL of DMF taken in a 250-mL three-necked round bottom flask equipped with a reflux condenser, dropping funnel, and a nitrogen inlet. To this, the synthesized epoxy-functionalized siloxane (1 mmol) was added slowly and refluxed at 60°C under nitrogen atmosphere for 6 h. Then the solvent was removed under vacuum to give the imide-functionalized polydimethylsiloxane. The unreacted reactants were removed by repeated washing with toluene.

Appearance of the following absorption bands in the FTIR spectrum confirmed the product formation in all the imides.

FTIR: 3259 cm^{-1} (OH and NH), 3058 cm^{-1} (aromatic stretch), 2181 cm^{-1} (Si—H), 1061 cm^{-1} (Si—O—Si), 1588 cm^{-1} (Ar C=C), 1286 cm^{-1} (Si—CH_3), 1154 cm^{-1} (C—O), 987 cm^{-1} (Ar. C—H out of plane bending), 1724 cm^{-1} (C=O in phase of imide), 1627 cm^{-1} (C=O out of phase imide), 1320 cm^{-1} (C—*N*—C of imide). Disappearance of peak at 907 cm^{-1} (epoxy ring stretch) confirmed the imide incorporation.

Figure 2(a,b) represents the ^{1}H and ^{13}C NMR, respectively, given for the PIS (A) as a representative spectrum for all the imides.

In the ^{1}H NMR (ppm) spectrum, 0.0 [Si—(CH_3)$_3$], 0.85 (Si—CH_2), 0.45 (—Si—CH_3), 3.2 (CH_2—O—CH_2), 4.1 (—O*H*), 2.8 (C*H*—OH), 3.4 (NH_2, broad), 1.7 (NH), 6–8 (aromatic protons). The disappearance of resonance signals at 2.6 and 3.2 ppm confirms the epoxy ring cleavage, and the appearance of chemical shift at 4.5 ppm confirms the presence of SiH. The chemical shifts corresponding to the imide groups were obtained in the regions as discussed in the imide synthesis.

^{13}C NMR (ppm): 0–15 (Si—CH_3), 64, 72 (CH_2—O—CH_2) and the chemical shifts were in the regions as discussed in the imide synthesis.

RESULTS AND DISCUSSION

Although some polyimides derived from fluorinated anhydride have been discussed previously, the utilization of these fluorine-containing polyimides in combination with the siloxanes is not well known. In this work, the 6FDA was reacted with three different

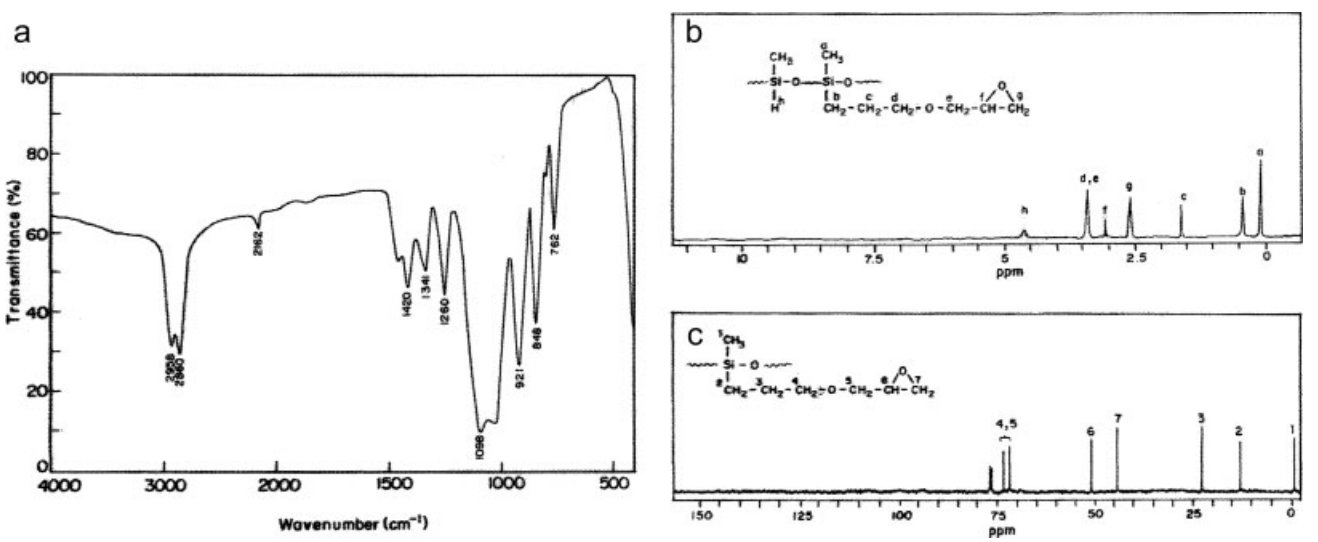

Figure 1 (a) FTIR spectrum of the epoxy-functionalized PDMS, (b) ^{1}H NMR spectrum of the epoxy-functionalized PDMS, and (c) ^{13}C NMR spectrum of the epoxy-functionalized PDMS.

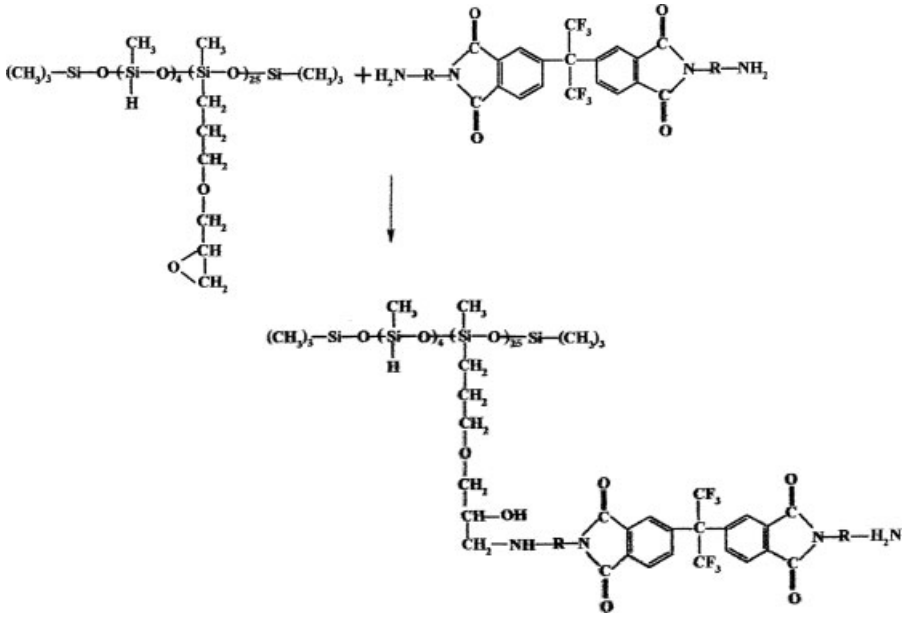

Scheme 3 Synthesis of poly(imide-siloxane)s.

amines (DDBP, DDM, and DBP) that are chosen to be the bulky and rigid units. This was chosen keeping in mind the influence of bulky rigid groups in controlling the permeability and selectivity for potential gas separations. These synthesized imides would have not been soluble in any of the common solvents if there were no fluorine groups present in them.

In this experiment, 25 mmol of allyl-3-epoxy propyl ether was reacted with 1 mmol of PHMS in the presence of platinum catalyst for 48 h in toluene medium. The number of Si—H groups present in the PHMS were found to be at an average of 29 units per molecule. From the NMR data it is found that one mole of PHMS reacted with 22 mol of allyl compound. The remaining seven Si—H groups per mole in the epoxy-functionalized PHMS were used for further crosslinking with hydroxy-terminated PDMS to form polydimethylsiloxane film containing imide moiety.

Solubility of amine end-capped imide

It is well-known that aromatic polyimides are insoluble in many conventional organic solvents, because of their highly conjugated, rigid-rod like chemical structures. The solubilities of the synthesized amine end-capped imides in a wide range of solvents of

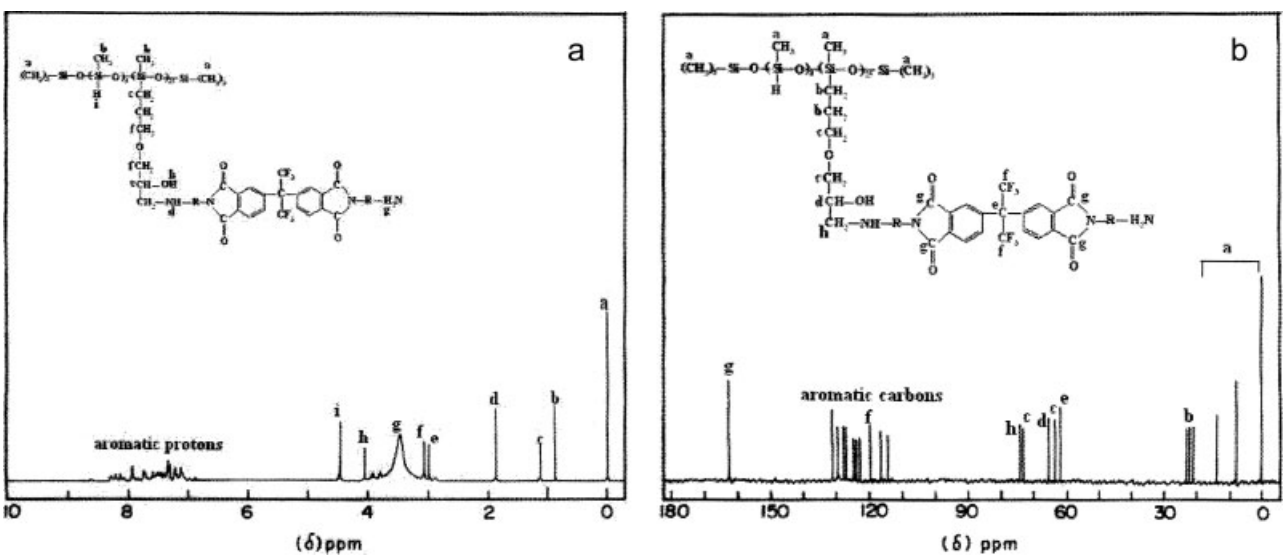

Figure 2 (a) ^{1}H NMR spectrum of PIS (A) and (b) ^{13}C NMR spectrum of PIS (A).

TABLE II
Solubility Behavior of Amine End-capped Imides[a]

Diamines	DMSO	DMF	Toluene	THF	EMK	Ethyl acetate	Chloroform
A	+	+	−	+h	+	+h	+h
B	+	+	−	+	+	−	−
C	+	+	−	+	+	−	−

NMP, *N*-methylpyrrolidone; DMAc, *N*,*N*′-dimethylacetamide; DMF, *N*,*N*′-dimethylformamide; EMK, ethyl methyl ketone; THF, tetrahydrofuran

Symbols: +, soluble at room temperature; +h, partially soluble on heating; −, Insoluble even on heating.

[a] Quantitative solubility was tested with 15-mg sample in 1 mL of solvent.

different polarities are given in the Table II. The solubility of the amine end-capped imides was qualitatively determined by the dissolution of 15-mg solids in organic solvents. All the three imides were found to be highly soluble in polar aprotic solvents like DMSO. In addition the high solubility was observed in ethyl methyl ketone (EMK). Imide system B shows extended solubility in THF and ethyl acetate. This improved solubility may be due to the presence of the methoxy groups attached to the aromatic rings in their ortho positions. Without being bound by any particular theory, the excellent solubility of the 6FDA-based polyimides may be attributed partially to the types of diamines used. The rigid diamines disrupt the chain packing, eliminate crystallinity, and interrupt conjugations along the chain backbones. The resulting loose packing generates more free volume, which permit solvent molecules to penetrate into the imide systems.

These imides were reacted with the epoxy-incorporated PHMS backbone via epoxy ring cleavage. To ensure the complete reaction of the imide with the epoxy-functionalized PHMS and to avoid the crosslinking reactions, the dilute siloxane oligomer was added dropwise to the bulk of the imide solution. The resulting PIS were highly soluble in EMK which is a favorable property for casting the film, and this showed high compatibility with siloxane. The intrinsic viscosities calculated in DMF solvent were found to vary between 0.32 and 0.45 dL/g.

Thermal properties

The thermal degradation pattern of the PDMS and the epoxy-functionalized siloxane without hard imide segments were examined for comparison with the PIS systems to understand the improvement in the thermal stability achieved by the incorporation of the hard imide groups. The thermograms in the Figure 3 show the thermal degradation pattern observed for all the three PIS systems. The systems without the imide groups show single-stage decomposition. The epoxy-functionalized PHMS show an initial degradation at 250°C. All the three PIS systems showed almost similar degradation with distinct three-step decompositions. The more or less similar pattern may be due to the close similarity in the structural backbone of the imide groups. The first step decomposition was observed around 215°C, and this may be attributed to the decomposition of the aliphatic groups connecting the imide and the siloxane backbone. It is reported that the aliphatic *n*-propyl segments have less thermo-oxidative stability.[28] Even though the initial degradation starts slightly earlier than the PDMS, the long-term thermal stability was observed with the incorporation of the imide groups in the PIS systems. The limited long-term thermal stability of these systems could be caused primarily by the degradation of the siloxane backbone as they are easily susceptible to ionic reactions. PDMS thermally decomposes to cyclic oligomers through Si—O bond scission in a chain-folded cyclic conformation energetically favored by overlapping of empty silicon d-orbitals with the orbitals of the oxygen and carbon atoms.[29] The second stage of the decomposition was observed around 390°C which could be due to the degradation of the siloxane backbone, and the decomposition of the imide

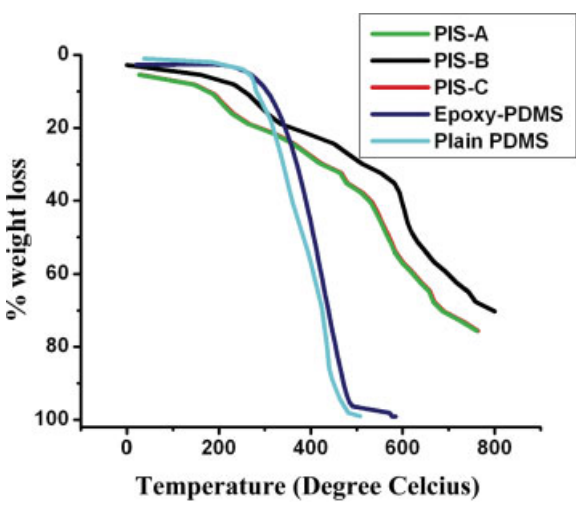

Figure 3 TGA analysis for the imide systems. [Color figure can be viewed in the online issue, which is available at www.interscience.wiley.com.]

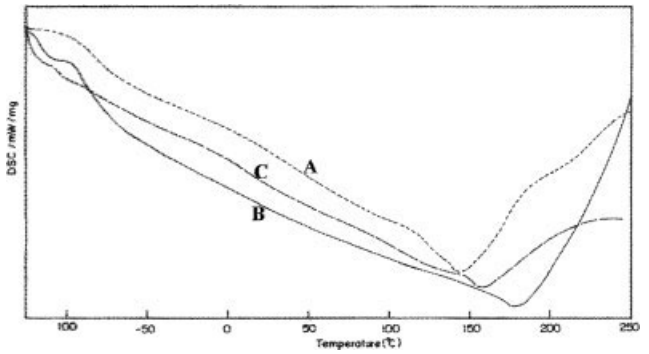

Figure 4 DSC analysis for the imide systems.

groups was observed around 565°C which shows the higher thermal stability observed for these rigid imide groups. All the systems showed a char yield value of 18% at 750°C.

Differential scanning calorimetry

The transitions occurring under the thermal conditions are recorded in the DSC spectrum for all the three PIS systems and are presented in Figure 4. The observation of the DSC spectrum clearly shows two distinct transitions for all the three PIS systems. One transition is observed at the lower end in the negative temperature and the other transition at the higher end. The T_g for the epoxy-functionalized PHMS was observed to be −118°C which is higher when compared with unmodified PHMS which showed T_g at −123°C. It is well-known that the Si—O—Si linkages show a flexible nature which will enhance the mobility of the chains thereby marking its glass temperature value to −123°C. Among the three PIS systems, PIS (B) shows the lowest transition at −107°C followed by the systems PIS (A) and

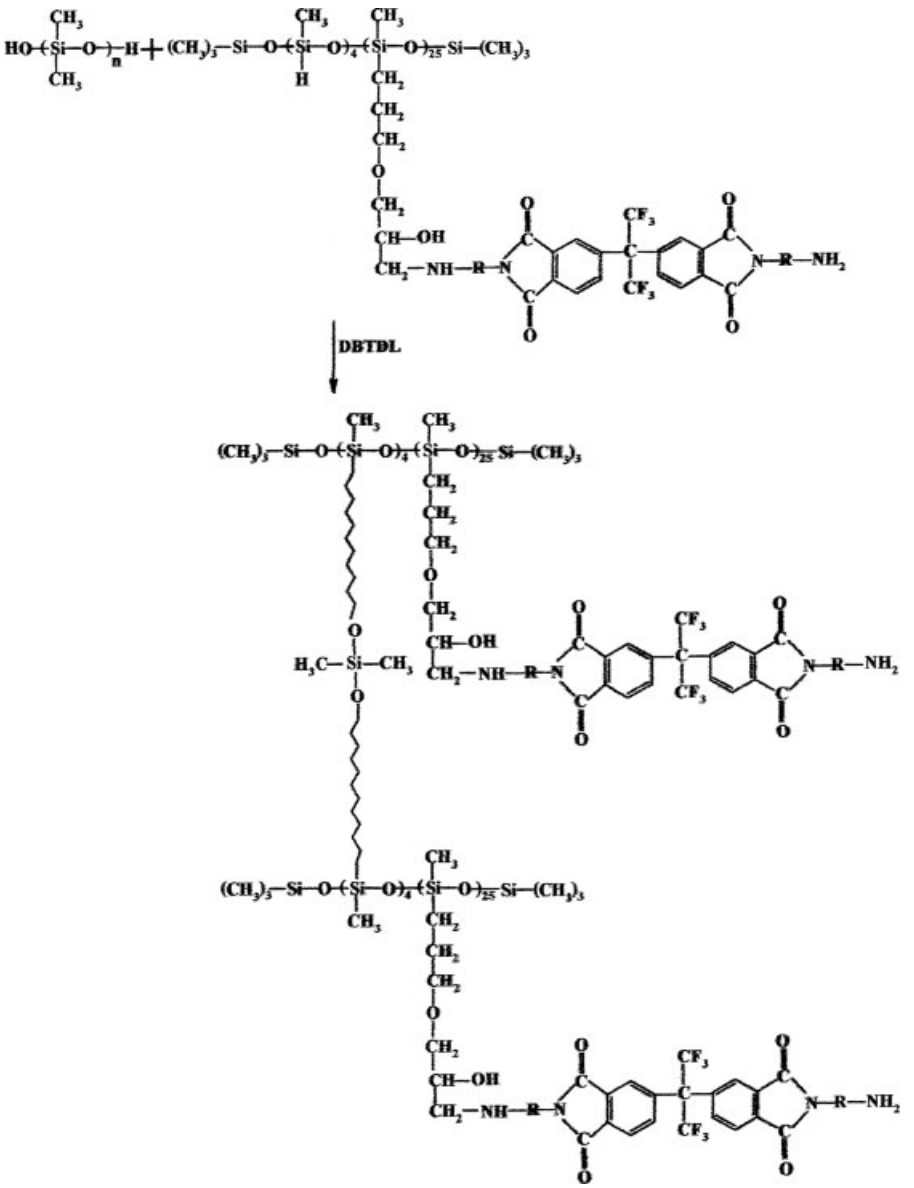

Scheme 4 Synthesis of PIS membranes.

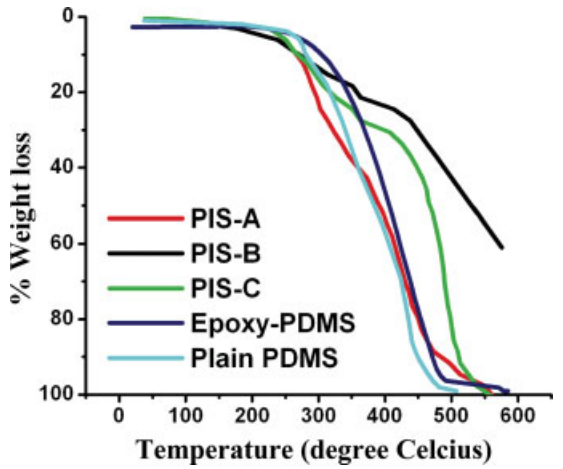

Figure 5 TGA analysis for the PIS systems. [Color figure can be viewed in the online issue, which is available at www.interscience.wiley.com.]

PIS (C) at −88 and −81°C, respectively. The transition in these systems observed at these negative temperatures could be attributed to the T_g of siloxane backbone, and the shift in the observed T_g from −123°C to higher temperatures is because of the presence of rigid imide groups which intervenes in the mobility of the flexible groups. The second transition is observed in all the three PIS systems (A, B, and C) at 145, 174, and 152°C. This variation in the T_g of the imides is in accordance with their rigidity. The existence of two distinct T_gs for the soft and hard segments suggests that the two segments are phase separated in all the three PIS systems. PIS (B) which shows much lower T_g for the soft segment and a higher T_g for the hard segment could be thought of more phase separated among the three systems.

Film formation

Imide-incorporated PDMS films were synthesized by solution curing method using hydroxyl-terminated PDMS. The high-molecular weight hydroxyl-terminated PDMS was obtained by the ring-opening reaction of octamethylcyclotetrasiloxane using potassium hydroxide. Synthesis of imide-incorporated polydimethylsiloxane is shown in Scheme 4. PDMS films containing different concentrations of imides were prepared by mixing 5, 10, 15, and 20 wt % of PIS (A or B or C) with respect to the hydroxyl-terminated PDMS in EMK/toluene mixture (1 : 3 v/v). The seven free Si—H groups present in the imide-incorporated PDMS crosslinks with the hydroxyl-terminated PDMS. A few drops of di-*n*-butyltindilaurate catalyst were added to facilitate the coupling reaction. Then the solution was poured into the Teflon-coated glass plate. After the solvent was evaporated, a thin dense film with thickness ranging from 100 to 200 μm was peeled from the glass plate and the thickness was measured using a digital micrometer. The homogenous films obtained with 20 wt % PIS (A, B, and C) incorporations were tested for their thermal, mechanical, and surface properties.

Thermal characteristics of the films

The thermal stability of the synthesized films containing 20 wt % PIS was studied by the thermogravimetric analysis and is represented in Figure 5. All the three systems showed two stages of decompositions. The first stage decomposition was observed at 240°C for PIS (A), and around 312°C for PIS (B) and PIS (C). This could be attributed to the decomposition of the siloxane groups present in the network. We could observe a difference in the decomposition temperature of siloxane groups in the PIS systems and the PIS films. This increase in the decomposition temperature is because of the crosslinked structure in the networks. PIS (B) shows an earlier start of decomposition even at 150°C because of the siloxane groups which may be attributed to the higher phase separation observed as from DSC. The second decomposition temperature is observed at 403, 455, and 436°C for PIS (A), (B), and (C), respectively. In this also, PIS (B) shows the highest value, which could be due to the same reason of higher phase separation and increased structural rigidity. The DSC curves for the crosslinked networks are given in Figure 6. There are three transitions observed in the DSC for all the three PIS films (Table III). The lowest transition around −100°C could be attributed to the T_g of the siloxane groups present in the film. The reduced segmental chain mobility of the siloxane units could be observed from the reduction in the T_g values when compared with PIS systems. The sharp endotherm observed at −43°C in all these systems is a new transition, which is not observed in the uncrosslinked systems. It is reported that the PDMS matrix shows the melting endotherm around

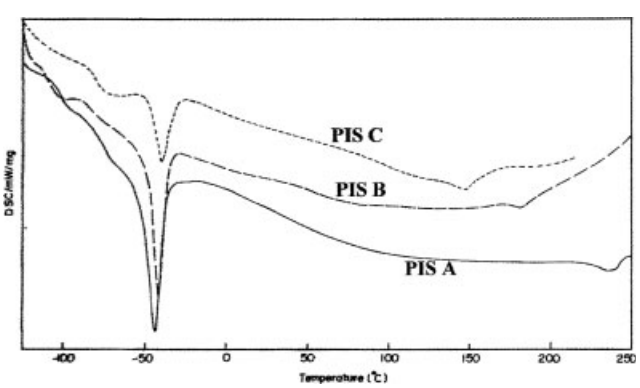

Figure 6 DSC analysis for the PIS systems.

TABLE III
Thermal and Mechanical Properties of the PISs

Sample	[η] (dL/g)	Onset of maximum decomposition temperature (°C)	T_{50} (°C)	%Char yield	T_{g1} (°C)	T_{g2} (°C)	T_m (°C)	Tensile strength (MPa)	%Elongation at break	Density
PIS (A)	0.375	285	430	21	−100	170	−43.1	93	70	1.17
PIS (B)	0.450	298	470	20.9	−107	239	−40.1	90	65	1.9
PIS (C)	0.32	292	453	23	−101	162	−42	87	81	1.2

−45°C.[30] In the networks that we have prepared, the crosslinking is carried out with the PDMS matrix whose melting point may be observed at −43°C which is not observed in the uncrosslinked systems where PDMS matrix is not present. A mild transition is observed in the higher end of the thermogram for all the systems around 230°C. The observation of two distinct glass transition temperatures is indicative of the possible microphase-separated structures containing microdomains of hard imide and soft siloxane segments. The confirmation of this observation and the sizes of the agglomerates will be discussed in the SEM analysis.

The DMA is an efficient tool to measure the network structure, morphology, and thermomechanical properties of the network system. Figure 7(a) shows the storage modulus and Figure 7(b) shows the loss factor (tan δ) against temperature for the films.

From the storage modulus data, it is observed that all the three systems showed a sharp drop in the storage modulus value followed by a plateau as the temperature increased. This region is the transition region where the polymer changes from glassy state to rubbery state. This behavior is attributed to the segmental mobility of polymer chains in that region. The appearance of the plateau at the higher temperature indicates that stable crosslinked network exists.[31] The differences in the storage modulus for the various systems are related to the different crosslinking densities. The lowest crosslinking density results in the lowest T_g and the lowest storage modulus. The lowest storage modulus of 800 MPa was observed in the case of PIS (C) when compared with PIS (A) that shows a value of 1200 MPa and PIS (B) shows 1400 MPa. The presence of rigid biphenyl imide groups present in PIS (B) is responsible for the observed highest storage modulus. This is followed by the PIS (A) and PIS (C) that also has rigid groups, but with maximum phase mixing with the flexible siloxane groups shows reduced storage modulus values.

The discussion of the loss factor gives the measure of the energy loss in a sample subjected to a small sinusoidal stress.[32] A maximum value in the tan δ against temperature plot is generally observed around T_g. All the systems showed two peaks—one in the lower end and the other at the higher temperature. For PIS (B) the second peak was very sharp corresponding to the higher phase separation, whereas in PIS (A) and PIS (C) the peak was not very sharp. In PIS (B) the lower end T_g value was observed at −80°C, and the transition was observed over a shorter range between −100 and 0°C. For PIS A and PIS C the T_g was observed at −81 and

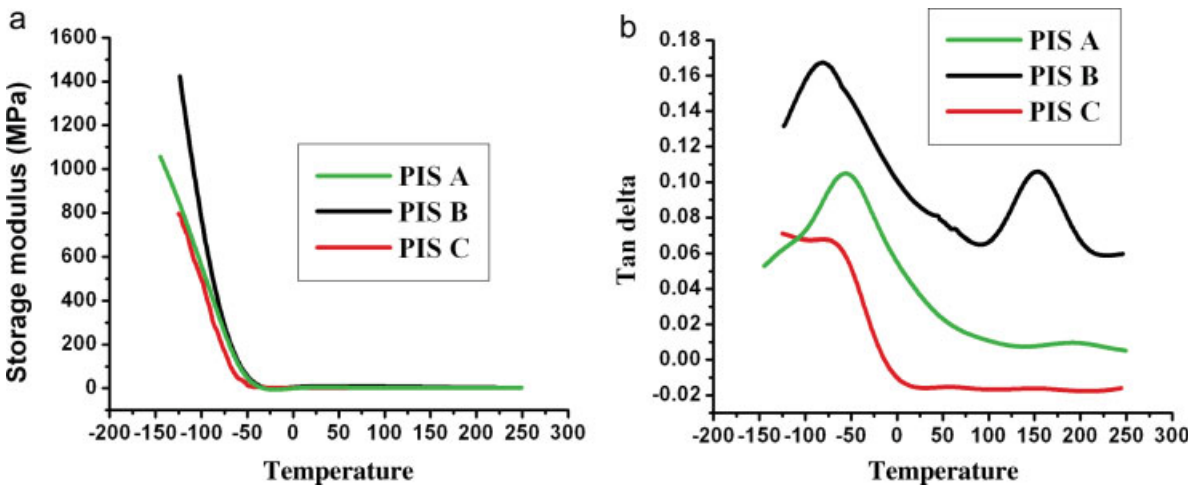

Figure 7 (a) Storage modulus for the PIS systems and (b) tan δ for the PIS systems. [Color figure can be viewed in the online issue, which is available at www.interscience.wiley.com.]

−55.9°C, respectively. In both these cases, the transition was observed over broader range between −100 and 80°C. The higher end T_g in PIS (B) was observed around 200°C corresponding to the rigid imide groups. The area under the curve shows the extent of phase mixing with the sharp tan δ peak, and the sudden drop in storage modulus corresponds to complete phase separation.[33]

The densities of the synthesized PIS films are given in Table III. Generally a higher decrease in density is observed with the rigid groups, which hinder chain packing. In all the three PIS systems the bulky —C(CF_3)— groups are present which obstruct the chain packing resulting in higher density. Also in all the systems, rigid groups like biphenyl groups are present and therefore resulting in more or less equal density values between 1.17 and 1.22 g/cm^3.

The tensile properties of the 20 wt % PIS films were studied and the results are given in Table III. The most important observation from the tensile strength data is that the PIS (B) film containing rigid biphenyl groups showed the low-tensile strength value of 90 MPa with 65% elongation at break when compared with PIS (A) that showed a tensile strength of 93 MPa. This observation could be explained on the basis of higher phase separation of the PIS (B) film that is very clear from the DSC and DMA analysis. This phase separation could be the reason for the reduced tensile strength values, as the rigidity is not contributing much to the strength in combination with the siloxane groups. The combination of the soft siloxane and hard imide groups gives the optimum mechanical strength, which is sufficient for the gas separation applications.

WAXD measurements

Even though there are alternative approaches to determine the phase composition including density measurements, thermal analysis, and spectroscopy, XRD remains the most robust and simplest technique and so it is of dominant importance. Figure 8 shows the wide-angle X-ray diffraction pattern observed for the PIS films with 20% incorporation. The *d*-spacing value in the diffraction pattern characterizes the chain to chain distance in the polymer matrix. This was calculated using the Bragg's equation

$$2d \sin \theta = nl$$

This method has been used to determine the interchain distance in the amorphous systems by measuring the θ-value at maximum intensity in the amorphous scattering region. The amorphous halo will give rise to a broad band implying a *d*-spacing distribution. All the PIS films showed typical diffraction peaks at 2θ varying between 11.3° and 12.5°. There was no sharp peak observed in any of these films. The haloes observed could be due to the amorphous structure or presence of crystalline structure.[34] Since the DSC results did not show any endothermic peak at the temperature of WAXD experiments, the halo could be assigned to the amorphous nature of the films. The most prominent peak in the amorphous polymer spectra is often used to estimate the average interchain spacing distance (*d*-spacing). These values were calculated using the Bragg equation and were found to be 7.189 Å for PPIS (A), 6.753 Å for PPIS (B), and 7.001 Å for PPIS (C). PIS (B) shows the highest *d*-spacing value because of the bulkiness of the methoxy biphenyl groups which is followed by PIS (A). The *d*-spacing for PIS (C) shows the lowest value probably because of the close alignment of the polymer.

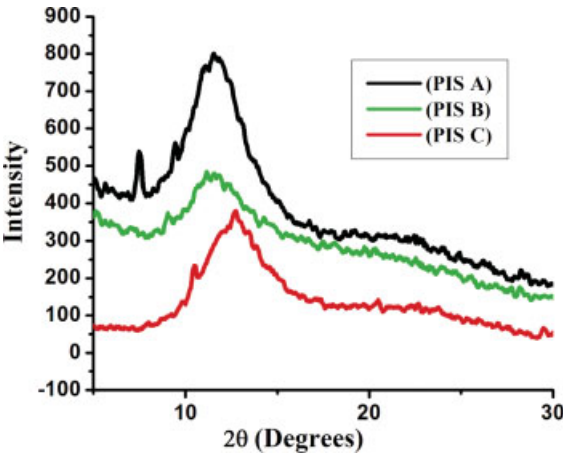

Figure 8 WAXD spectra of crosslinked PIS membranes. [Color figure can be viewed in the online issue, which is available at www.interscience.wiley.com.]

Contact angle measurements

It has been suggested that amorphous, comb-like polymers possessing a flexible linear backbone, onto which are attached side chains with low intermolecular interactions, will exhibit low surface energy.[35] It is well-known that the surface energy decreases drastically in the siloxane-containing compounds. In addition, the fluorinated groups also reduce the surface tension of resulting compound. The more flexible fluorosiloxanes exhibited surface energy values of 12–17 mN/m, but was not found to be further reduced than this value. This observation may be rationalized at the submolecular level that the materials display different molecular organization characteristics at the film air interface. There is a preferential distribution of the siloxane backbone nearer to

TABLE IV
Surface Energies of the PIS Membranes

Sample	%PIS	γ_s^d mN/m	γ_s^p mN/m	γ_{SV} mN/m
PIS	0	16.7	5.8	22.6
PIS (A)	5	21.0	6.2	27.2
	10	8.9	12.4	21.3
	15	10.5	8.8	19.3
	20	13	3.5	16.5
PIS (B)	5	24.73	16.35	41.08
	10	23.24	13.5	36.74
	15	22.16	10.2	32.36
	20	22.02	9.8	31.82
PIS (C)	5	18.4	9.6	28
	10	17.9	8.2	26.1
	15	17.0	6.5	23.5
	20	16.2	5.2	21.4

the surface with the pendent perfluorocarbon chains oriented toward the bulk of the sample.[36,37]

The contact angle measurements provide information about the surface energies of the system. The polar and dispersion factors were calculated using the following Young and Fowkes[38] equation:

$$\gamma_{LV}(1+\cos\theta) = 2(\gamma_L^d\gamma_s^d)^{1/2} + 2(\gamma_L^p\gamma_p^s)^{1/2}$$

where γ_{LV} is the interfacial tension at liquid/air interface, γ_L^d and γ_s^d are the dispersion factors of the sample for liquid and solid respectively, γ_L^p and γ_s^p are the polar factors of the sample for liquid and sample, θ is the contact angle between the sample and liquid/air interface. The total surface energy γ_{SV} of the samples were estimated using the following relationship:

$$\gamma_{SV} = \gamma_S^d + \gamma_S^d$$

The angle of contact between water and octadecane for all the films were measured and it is given in the Table IV. The total surface energy of the PIS film without any imide shows the minimum surface energy of 22.6 mN/m. All the three systems show the higher surface energy values when compared with the plain PIS film even though hydrophobic fluorine is present in all the systems with flexible siloxane backbone. This could be attributed to the crosslinked nature of the film with the rigid groups that might prevent the free mobility of the hydrophobic groups to lower the surface energy. It could be substantiated from the highest surface energy values for PIS (B) which has the very rigid biphenyl units that also showed maximum phase separation. This is followed by PIS (A) with diaminodiphenyl units and PIS (C) with benzophenone imide groups. It is seen in all the systems that with increase in the percentage incorporation of the PIS in the film results in the decrease in the surface energy because of the availability of more number of fluorine groups. In each of these systems, the increase in the PIS alters the polar factor much more than the dispersion factor. This shows the sensitivity of the polar factor to the fluorine groups.

Surface morphology

SEM pictures for the three systems containing 20% PIS are given at two different magnifications [Fig. 9(a–c)] to study their morphology. All the three

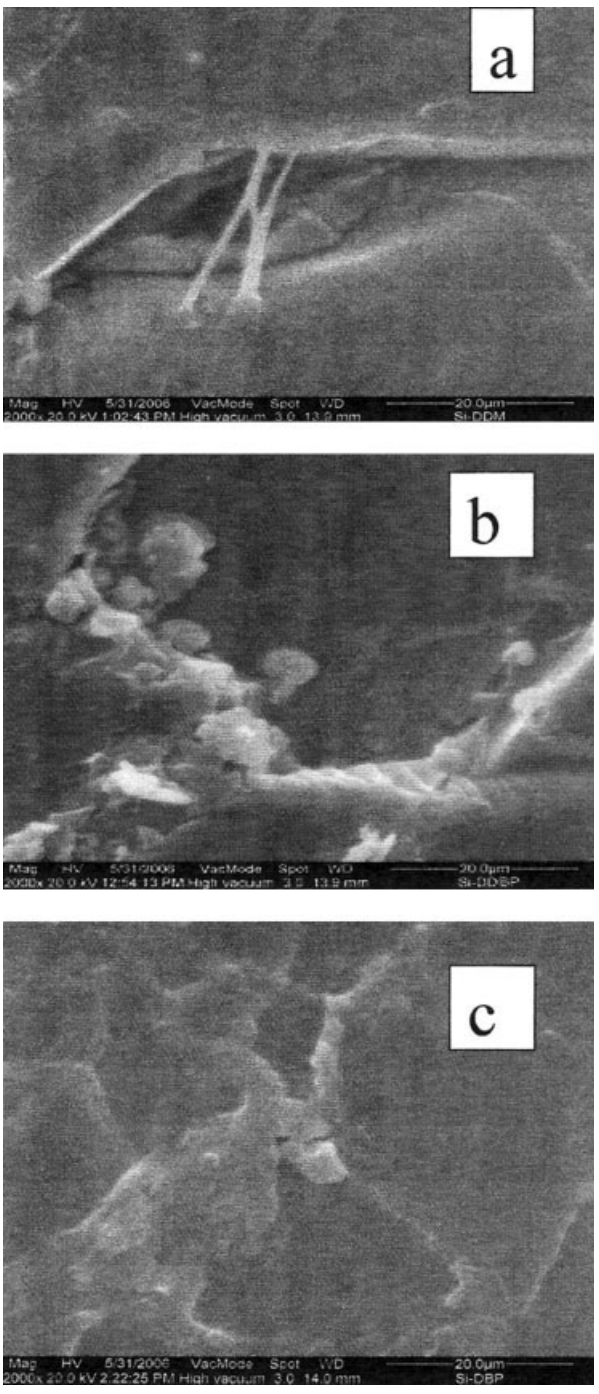

Figure 9 (a–c) SEM pictures for the PIS systems.

systems show phase-separated morphology with agglomerate-like structures that are seen at higher magnifications. There were no voids observed in any of these systems. The PIS (A) shows string-like structures at some portions which could be corroborated to the improved mechanical properties. The PIS (A) and PIS (C) systems does not show complete phase separation having globule like structures but show some aggregated curls that mix with the background. This shows the partial miscibility of the hard and soft segments with retardation on the mobility of the large hard segment because of the rigid crosslinking and thus, enhancing the domains of the hard imide segment seen as curls.

CONCLUSIONS

This work dealt with the synthesis of PIS containing highly rigid imide groups whose excellent solubility is achieved by the introduction of fluorine groups. The synthesized PIS systems were observed to be thermally very stable and possess two distinct phases as observed from the DSC. It was also observed that the presence of hard segments decreases the mobility of the soft segments, thereby increasing the T_g of siloxane from -123 to -80°C. The improved solubility of the PIS systems facilitated the preparation of poly(imide-siloxane) films by crosslinking with the higher molecular weight polydimethyl siloxane. These films also showed high thermal stability in combination with the high-molecular weight siloxane and also showed phase separation which was further confirmed by the DMA. Depending upon the rigidity of the imide groups, the storage modulus varied and there was shift in their respective glass transition temperatures. This phase separation was further confirmed from the SEM analysis which showed curled agglomerated structures suggesting the inhibition in mobility of the hard segments to get homogenized with the soft segments. The films also showed high-tensile strengths when compared with the polydimethylsiloxanes because of the incorporation of the hard imide segments to the siloxane backbone. The effect of the fluorine groups in the surface energies of the films were studied, and noted that the polar factor was much affected by the fluorine groups that reduces the surface energy. A maximum reduction in the surface energy to 21.4 mN/m was observed.

References

1. McGrath, J. E.; Wang, L. F.; Mecham, J. B.; Ji, Q. Polym Prepr 1998, 39, 455.
2. Clarson, S. J.; Semlyen, J. A., Eds. Siloxane Polymers; Englewood Cliffs, NJ: Prentice Hall, 1993.
3. Sheth, J. P.; Aneja, A.; Wilkes, G. L.; Yilgor, E.; Atilla, G. E.; Yilgor, I.; Beyer, F. L. Polymer 2004, 45, 6919.
4. Yilgor, J. E.; McGrath, J. E. Adv Polym Sci 1988, 1, 27.
5. Pu, Z.; Mark, J. E.; Li, Z.; Zhu, J. Polymer 1999, 40, 4695.
6. Liaw, D. J.; Chang, F. C. J Polym Sci Part A: Polym Chem 2004, 42, 5766.
7. Ghosh, M. K.; Mittal, K. L., Eds. Polyimides, Fundamentals and Applications; Marcel Dekker: New York, 1996.
8. Simionescu, M.; Marcu, M.; Cazacu, M. Eur Polym J 2003, 39, 777.
9. Arnold, C. A.; Summers, J. D.; Chert, Y. P.; Bott, R. H.; Chen, D.; McGrath, J. E. Polymer 1989, 30, 986.
10. Hergenrother, P. M.; Havens, S. J. J Polym Sci Part A: Polym Chem 1989, 27, 1161.
11. Hergenrother, P. M.; Beltz, M. W.; Havens, S. J. J Polym Sci Part A: Polym Chem 1991, 29, 1483.
12. Hougham, G.; Tesoro, G.; Shaw, J. Macromolecules 1994, 27, 3642.
13. Brink, M. H.; Brandom, D. K.; Wilkes, G. L.; McGrath, J. E. Polymer 1994, 35, 5018.
14. Rogers, M. E.; Brink, M. H.; McGrath, J. E.; Brennan, A. Polymer 1993, 34, 849.
15. Wirth, J. G. In High Performance Polymers: Their Origin and Development; Seymour, R. B.; Kirshenhaum, G. S., Eds. Elsevier: Amsterdam, 1986, 45.
16. Jin, Q.; Yamashita, T.; Horie, K. J Polym Sci Part A: Polym Chem 1994, 32, 503.
17. Auman, B. C.; Highley, D. P.; Scherer, K. V., Jr.; McCord, E. F.; Shaw, W. H. Polymer 1995, 36, 651.
18. Harris, F. W.; Sakaguchi, Y. Polym Mater Sci Eng 1987, 60, 187.
19. Mikroyannidis, J. A. Macromolecules 1995, 28, 5177.
20. Huang, S. J.; Hoyt, A. E. Trends Polym Sci 1995, 3, 262.
21. Shimazu, A.; Miyazaki, T.; Matsushita, T.; Maeda, M.; Ikeda, K. J Polym Sci Part B: Polym Phys 1999, 37, 2941.
22. Lin, W. H.; Vora, R. H.; Chung, T. S. J Polym Sci Part B: Polym Phys 2000, 38, 2703.
23. Yamada, Y.; Furukawa, N.; Tujita, Y. High Perform Polym 1997, 9, 145.
24. Holmberg, K., Ed. Handbook of Applied Surface and Colloid Chemistry. Wiley: England, 2002; Vol. 2, p 256.
25. ASTM. In ASTM Annual Book of Standards D-792; ASTM: West Conshohocken, PA, 1993.
26. Senthilkumar, U.; Reddy, B. S. R. J Membr Sci 2004, 15, 73.
27. Paul, S.; Ranby, B. Anal Chem 1975, 47, 1428.
28. Sun, Y.; Liu, Y. G.; Yin, J.; Gau, J.; Zhu, Z. K.; Hang, D. Y.; Wang, Z. G. J Polym Sci Part A: Polym Chem 1999, 37, 4330.
29. Camino, G.; Lomakin, S. M.; Lazzari, M. Polymer 2001, 42, 2395.
30. Yang, H.; Nguyen, Q. T.; Ping, Z.; Long, Y.; Hirata, Y. J Mater Res Innovat 2001, 5, 81.
31. Li, F.; Larock, R. C. Polym Adv Technol 2002, 13, 436.
32. Rababi, G.; Kraft, A. Macromol Rapid Commun 2002, 23, 375.
33. Nielsen, L. E. Mechanical Properties of Polymers and Composites; Marcel Dekker: New York, 1974.
34. Billmeyer, W. F. Jr. Textbook of Polymer Science; Wiley: Singapore, 2000; p 238.
35. Owen, M. J. Comments Inorg Chem 1988, 7, 195.
36. Tsibouklis, J.; Stone, M.; Thorpe, A. A.; Graham, P.; Ewen, R. J.; Nevell, T. G. Langmuir 1999, 15, 7076.
37. Kassis, C. M.; Steehler, J. K.; Betts, D. E.; Guan, Z. B.; Romack, T. J.; DeSimone, J. M.; Linton, R. W. Macromolecules 1996, 29, 3247.
38. Adamson, A. W. Physical Chemistry of Surfaces; Interscience: New York, 1960.